

# Degenerate mirrorless lasing in thermal alkali vapors

Aneesh Ramaswamy\* and Svetlana A. Malinovskaya

*Stevens Institute of Technology, Hoboken, NJ, USA*

(Dated: March 20, 2025)

## Abstract

For a degenerate two-level alkali atom system driven by a linearly polarized continuous-wave pump field, the steady-state gain for an orthogonally polarized probe field was theoretically predicted [1]. Using linear response theory, we calculated the probe absorption spectrum when the pump was detuned from resonance. A sub-natural linewidth dispersive structure was observed near the pump resonance, exhibiting both gain and absorption. Additionally, a distinct pure gain peak appeared at a sideband corresponding to a dressed-state transition. These effects typically do not persist outside the ultracold regime due to inhomogeneous broadening caused by Doppler broadening, which washes out the fine spectral details. We demonstrate that the sideband gain peak is sustained in the warm vapor regime when both the pump Rabi frequency and detuning exceed the Doppler width,  $\Omega_P > \Delta_P \gg \Delta_{\text{Dop}}$ . Our results can enable degenerate mirrorless lasing in thermal alkali atom vapors, offering a significant enhancement in the signal-to-noise ratio for fluoroscopic remote magnetic sensing applications.

## I. INTRODUCTION

Mirrorless lasing is the generation of amplified light in the absence of mirrors or a resonator, relying purely on the properties of the gain medium. In this work, we consider the case of mirrorless lasing without a feedback loop (such as the one generated by scattering), focusing on the specific case of degenerate mirrorless lasing. In this case, a linearly polarized, strong continuous-wave pump field is used to drive an optical transition between two hyperfine levels of an alkali atom. Under specific values of the pump intensity and detuning, a strong directional emission can be generated with orthogonal polarization to that of the pump, involving the same two levels and at a frequency that is nearly degenerate with that of the pump. The physical processes and conditions realizing this phenomenon were explored in a previous work- and the results strongly implied that stimulated emission processes involving bare-state population inversion were not responsible for the presence of optical gain, suggesting the involvement of lasing without inversion [1].

Lasing without inversion (LWI) has been rigorously investigated in the last few decades, demonstrating profound applications for sensing and the generation of short-wavelength light in conditions where population inversion cannot be reliably generated [2]. One of the key areas where LWI showed promise was in the context of coherently driven atomic systems where a strong continuous-wave field was used to generate large atomic coherences and additional harmonics in the atomic spectra. These coherences can result in a breaking of the symmetry between absorption and stimulated emission at certain frequencies, leading to the observation of LWI. The optimal way to understand LWI is in the dressed state basis, representing the energy eigenstates of the atom and strong driving field [3]. Transitions between dressed states accurately reproduce the peaks in the emission and absorption spectra of the strongly driven atom. The features of ‘hidden inversion’ (population inversion in the dressed state basis) and oscillating coherences between dressed states were determined to be responsible for the generation of gain sidebands and central dispersive gain features respectively in the non-degenerate two-level system (TLS) [4]. Experimental observations have confirmed the presence of sideband gain [5, 6] and central dispersive gain for the TLS [4]. For the case of the system studied in this work, a similar relation was shown between population inversion in the dressed state basis and peaks in the theoretical and experimental

---

\* Contact author: aramasw1@stevens.edu

absorption spectrum [7].

While these gain features have been observed experimentally in the cold vapor regime (or with a collimated atomic beam), the presence of the atomic velocity distribution in the warm vapor regime leads to a washing out of the fine spectral gain feature, as Doppler shifts from atoms traveling with different velocities lead to interfering spectral responses. In addition, the spectral response is strongly dependent on the direction of the output field, since the spectral response varies as a function of the relative Doppler shift between the pump and output  $(\vec{k}_P - \vec{k}_O) \cdot \vec{v}$ . In this work, we demonstrate that in the limit where both the pump Rabi frequency and detuning exceed the Doppler width,  $\Omega_P > \Delta_P \gg \Delta_{\text{Dop}}$ , optical gain can be sustained at a sideband transition for cases where the probe is either co-propagating or counter-propagating with the output. This result has strong implications for applications in remote sensing, as the presence of amplification for a counter-propagating field can enhance metrics such as the signal-to-noise ratio and sensitivity, leading to significant enhancements in schemes such as laser guide star based magnetometry [8].

## II. THEORETICAL MODEL

We consider a vapor cell with absorbing walls, filled with a vapor of Rb-85 atoms with volume density  $n$  and temperature  $T$ , see Fig. 1. We introduce a forward propagating continuous-wave (CW) classical pump field with electric field strength  $E_P$  and frequency  $\omega_P = \omega_0 + \Delta_P$ , where  $\omega_0$  is the rest frame  $D_2[F = 2 \rightarrow F' = 3]$  transition frequency and  $\Delta_P$  is the pump detuning. The pump propagates in the  $\hat{y}$  direction with linear polarization  $\hat{x}$  and Rabi frequency is given by  $\Omega_P = -\hbar^{-1}d^{(z)} [F = 2, F' = 3] E_P$ . We choose the quantization axis to be  $\hat{z}$  such that the pump drives transitions  $|F = 2, m\rangle \rightarrow |F' = 3, m\rangle$ . Our goal is to determine the steady-state spectral response of the optically pumped vapor for a CW field, propagating in the  $\pm\hat{y}$  direction with polarization  $\hat{x}$  and with field strength  $E_G$ , that drives transitions  $|F = 2, m\rangle \rightarrow |F' = 3, m \pm 1\rangle$ . We will calculate the fluorescence spectrum  $g_E(\omega)$  and the weak-field absorption spectrum  $g_A(\omega)$  [9].

To model the vapor dynamics for a thermal vapor, we use the Lindblad master equation  $\frac{d\rho(\vec{v}, t)}{dt} = \mathcal{L}(v)(\rho(\vec{v}, t))$  with superoperator  $\mathcal{L}(v)$  for an atom with velocity  $\vec{v}$  in the lab frame. We consider the dynamics in the field interaction picture, where the transition dipoles are corotating with the pump field,

$$\mathcal{L}(v) = -\frac{i}{2\hbar} \sum_m [\Delta_P(\vec{v})\sigma_m^z(\vec{v}) + \Omega_{P,m}\sigma_m^x(\vec{v}), \cdot] + \sum_{\mu=x,z} \frac{\Gamma^{(\mu)}}{|d^{(\mu)}|^2} \mathcal{D}[d^{(\mu)-}(\vec{v})](\cdot) \quad (1)$$

Where we define quantities in the rest frame of the atom:  $\Delta_P(\vec{v}) = \Delta_P - \vec{k} \cdot \vec{v}$ , Pauli operators  $\sigma_m^a(\vec{v})$  for states with the same  $m$ ,  $\Gamma^{(\mu)}$  is the spontaneous decay rate for the  $F = 2 \rightarrow F' = 3$  transition with polarization  $\mu$ ,  $d^{(\mu)}$  is the transition dipole moment for the  $D2$  transition and  $d_m^{(\mu)}$  is the transition dipole moment for the transition starting from the ground state  $|F = 2, m\rangle$ ,  $\Omega_{P,m} = -\hbar^{-1}d_m^{(z)}E_P$  is the Rabi frequency for transitions between states with magnetic number  $m$ ,  $d^{(\mu)-}(\vec{v}) = \sum_m d_m^{(\mu)}\sigma_m^-(\vec{v})$  is the total dipole moment operator, and  $\mathcal{D}[X](\rho) = X\rho X^\dagger - \frac{1}{2}\{X^\dagger X, \rho\}$  is the Lindblad dissipator. The steady-state density matrix is given by  $\mathcal{L}(\vec{v})\rho_{ss}(v) = 0$ .

We are interested in modeling the radiative transfer of the output spectral intensity  $I_{\vec{k}}(z, t)$ , with wavevector  $\vec{k}$ , in the vapor cell.

$$\left(\frac{\partial}{\partial t} + \frac{1}{c}\frac{\partial}{\partial z}\right) I_{\vec{k}}(z, t) = \frac{n\hbar\omega_0}{4\pi|d^{(x)}|^2} (A(\omega_0) \langle g_E(\omega, \vec{v}) \rangle_V - B(\omega_0) \langle g_A(\omega, \vec{v}) \rangle_V) I_{\vec{k}}(z, t) \quad (2)$$

Where  $A(\omega_0)$ ,  $B(\omega_0)$  are the Einstein A and B coefficients for spontaneous and stimulated emission, respectively, and  $\langle g_X(\omega, v) \rangle_V = \int d^3v g_X(\omega, v) f_T(v)$  is the velocity averaged lineshape with Maxwell-velocity distribution  $f_T(v)$ . Eq. (2) is derived using the photon-number Heisenberg equations and only considering the first-order response. The emission and absorption spectra are derived from the two-point dipole correlation functions using the Heisenberg operators  $d_H^{(x)-}(v, t) = e^{(\mathcal{L}(v))^\dagger t} d^{(x)-}(v)$ ,

$$g_E(\omega, \vec{v}) = \int_0^\infty d\tau e^{-i(\omega - \omega_P - (\vec{k} - \vec{k}_P) \cdot \vec{v})\tau} \text{Tr} \left[ \rho_{ss} d^{(x)+}(v) d_H^{(x)-}(v, \tau) \right] \quad (3)$$

$$g_A(\omega, \vec{v}) = \int_0^\infty d\tau e^{-i(\omega - \omega_P - (\vec{k} - \vec{k}_P) \cdot \vec{v})\tau} \text{Tr} \left[ \rho_{ss} \left[ d_H^{(x)-}(v, \tau), d^{(x)+}(v) \right] \right] \quad (4)$$

In the weak field limit with near-resonant driving, the dynamics approximately follow the bare states  $|F, m\rangle$ ,  $|F', m\rangle$ . It then follows that the emission and absorption spectra approximately depend on the excited state populations  $\langle d^{(x)+}(v) d^{(x)-}(v) \rangle$  and population inversions  $\langle [d^{(x)-}(v), d^{(x)+}(v)] \rangle$  respectively. For our case, in the strong field off-resonant driving regime, the dynamics depends on the open system dressed states obeying

$\mathcal{L}(v)(\rho_{d,n}(v)) = -(\gamma_{d,n}(v) + i\nu_{d,n}(v))\rho_{d,n}(v)$ , and contributes to the presence of spectral peaks  $\propto \left(\gamma_{d,n} + i\left(\omega + \nu_{d,n} - \omega_P - \left(\vec{k}_p - \vec{k}_P\right) \cdot \vec{v}\right)\right)^{-1}$ . See Appendix A for details. This analytic form indicates the asymmetry between the co-propagating and counter-propagating pump-probe configurations because of the difference in the relative Doppler shifts. For our degenerate TLS scheme, the shift is  $\approx 0$  in the former case and  $\approx \pm 2\vec{k}_P \cdot \vec{v}$  in the latter case. Fig. 3 shows the cause of this apparent asymmetry in more detail. In the next section, we show numerical simulations of the spectral line-shapes, calculated using the QuTiP library. For calculation of the velocity-averaged lineshapes, we choose a finite number of velocity groups from the 1-D interval  $(-2v_{\text{dop}}, 2v_{\text{dop}})$  where  $v_{\text{dop}} = \sqrt{2k_B T/m_{\text{Rb}}}$  is the most probable speed.

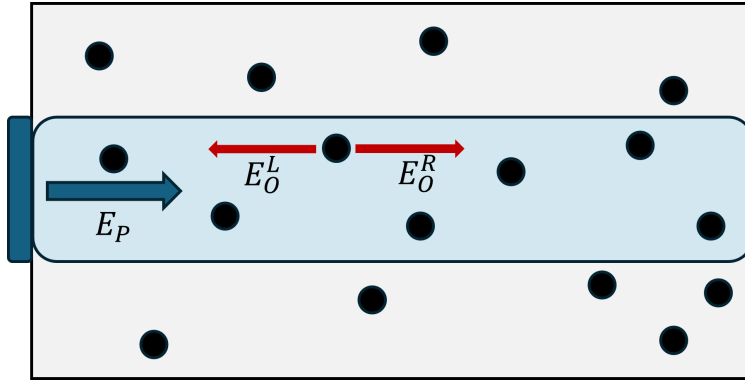


FIG. 1. Vapor cell configuration studied in this work. The cell has absorbing boundary conditions and is filled with Rb-85 atoms. A CW strong pump with field strength  $E_P$  is used to provide the conditions for degenerate mirrorless lasing for both left and right generated emissions.

### III. SPECTRAL RESPONSE

We first consider the simple case of an atomic vapor without a velocity distribution. In Fig. 4, we show the line-shapes in the strong field regime with  $\Omega_P = 4\Gamma$ , where  $\Gamma = (2\pi)6.0$  MHz, with off-resonant driving ( $\Delta_P = \mp\Gamma$ , left and right) and resonant driving (center). For the resonant case, we observe the presence of a central absorptive feature and two absorptive sidebands corresponding to dressed-state transitions split by the generalized Rabi frequencies  $\bar{\Omega}_m = \sqrt{\Delta_P(v)^2 + \Omega_{P,m}^2}/2$ . The latter is characteristic of the well-known Autler-Townes effect. We also observe a sub-natural linewidth enhanced absorption peak at

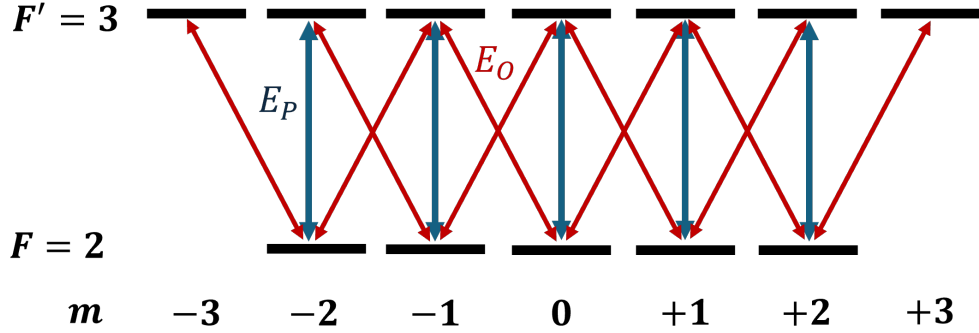


FIG. 2. Level scheme studied in this work. We use the Rb-85 D2 transition ( $F = 2 \rightarrow F' = 3$ ). The pump field  $E_P$  is  $z$ -polarized and drives same  $m$ -number transitions while the output field  $E_O$  is  $x$ -polarized.

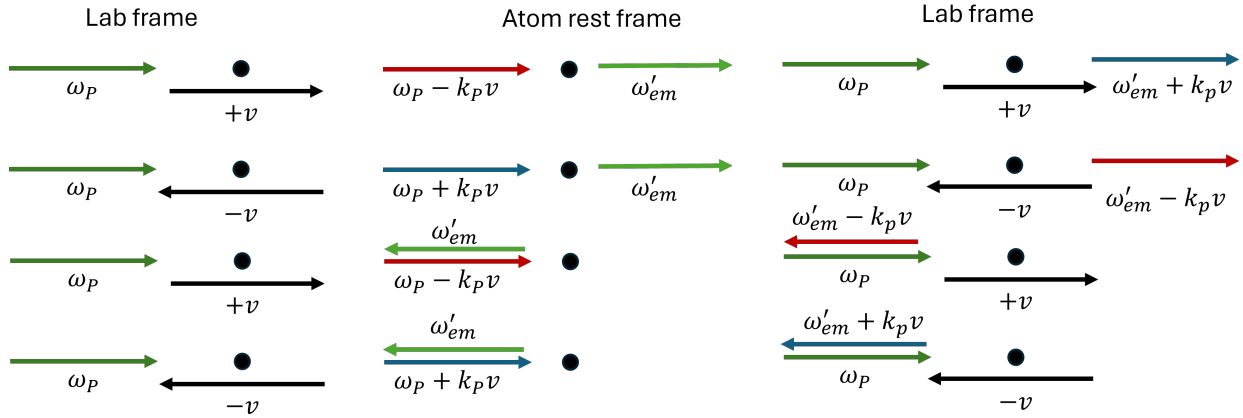


FIG. 3. Diagram showing the transformation of the pump and probe frequencies from the lab frame to the rest frame. The asymmetry of the relative Doppler shifts between the pump and emitted light for the co- and counter-propagating cases is a critical reason for the difference in the observed velocity-averaged spectral lineshapes.

the top of the central feature. This feature corresponds to the phenomena of electromagnetically induced absorption that occurs in systems with  $F' > F$ , due to optical pumping of the ground state population into the excited state sub-level with highest  $|m|$  [7]. In contrast to the phenomenon of electromagnetically induced transparency (EIT), which occurs as a result of destructive interference of scattering pathways, EIA is the result of constructive interference among near-degenerate (in frequency) dressed state transitions- leading to an enhancement of the dipole moment [10]. The EIA linewidth scales with the pump power

assuming that the pump field isn't strong enough to spectrally resolve the dressed-state transitions contributing to EIA.

In the off-resonant driving case, we observe the formation of the absorption and gain sidebands in  $g_A(\omega)$  that are characteristic of the Mollow triplet for the nondegenerate TLS- and reproduce the mirror symmetry of the spectral response when we flip the sign of  $\Delta_P$ . When we increase the detuning, the population moves between dressed states, leading to the presence of 'hidden inversion' in the dressed state basis and LWI gain. On the opposite side, enhanced absorption is observed as the movement of dressed-state population acts to increase absorption. We note that the gain sideband in  $g_A(\omega)$  coincides with an emission peak, implying that amplification of spontaneous emission (ASE) will occur- as indicated by Eq. (2). We would expect that as we increase the density  $n$ , we would observe the transition of a threshold for lasing-like behaviour, indicating degenerate mirrorless lasing.

We consider the central dispersive feature that replaces the EIA peak, exhibiting gain and absorption on opposite sides, which we call an Autler-Townes spike (AT spike). We distinguish this from the Autler-Townes doublet, which involves completely resolved spectral peaks corresponding to dressed state transitions that are nondegenerate in frequency such that interference between dressed state transitions is not a factor. Whereas the dispersive structure observed in the off-resonantly driven non-degenerate Mollow triplet is a result of oscillating dressed state coherences, the structure here has a contribution from 'hidden inversion' in the dressed state basis. The overlapping gain and absorption features can be explained as a result of insufficient spectral resolution of the dressed state transition peaks when  $\Omega_P$  isn't large enough. The lack of spectral resolution of these features implies that quantum interference phenomena, as in the case of EIA at resonant driving, also plays a part and further study is required to understand the contribution from both interference and 'hidden inversion'. As we increase  $\Omega_P$  further, the dispersive feature resolves into multiple spectrally resolved absorptive peaks as in the resonant driving case [7].

The presence of optical gain peaks is unfortunately lost when we introduce a thermal velocity distribution. Low temperatures in the sub 10 Kelvin range correspond to Doppler shifts of  $8.5\Gamma$ , leading to the cancellation of gain features due to the destructive interference in the spectral response from atoms travelling with different velocities. As observed in Fig. 5, the Doppler averaging leads to a complete suppression of optical gain and distinct dips about resonance are observed in the co-propagating case ( $\hat{k}_P \cdot \hat{k} = 1$ ). The contributions

about resonance in both spectra are primarily due to the velocity groups closest to zero as atoms with higher velocities are inefficiently driven due to large rest frame pump detunings  $\Delta_P(v) = \Delta_P - \vec{k}_P \cdot \vec{v}$ . The presence of relative Doppler shifts in the counter-propagating case leads to much broader spectral line-shapes as well as washing out of the central features observed in the co-propagating case.

The averaging out of gain is the result of overlapping contributions from the velocity-dependent spectral line-shapes that correspond to each of the three detuning cases in Fig. 4. In fact, if we choose  $|\Delta_P| \gg \Delta_{\text{Dop}}$ , we can ensure that only one set of qualitative characteristics is present for the majority of atoms in the velocity distribution. With this restriction, the spectral line shapes approximate functions that depend on only the frequency difference  $\delta(\omega, v) = \omega - \omega_P - (\vec{k} - \vec{k}_P) \cdot \vec{v}$ ,  $g_X(\omega, \vec{v}) \approx \tilde{g}_X(\delta(\omega, \vec{v}))$ . With this condition on  $\Delta_P$ , the velocity-averaged line-shapes for the co- and counter- propagating cases become,

$$\langle g_X(\omega, \vec{v}) \rangle_{V, \text{co}} \approx \tilde{g}_X(\omega - \omega_P) \quad (5)$$

$$\langle g_X(\omega, \vec{v}) \rangle_{V, \text{cn}} \approx \int d^3v f_T(v) \tilde{g}_X(\omega - \omega_P + 2\vec{k}_P \cdot \vec{v}) \quad (6)$$

This result is supported by our remark on the asymmetry of the relative Doppler shift for the two propagating cases. With sufficiently large detuning, provided we choose appropriate parameters to observe a gain sideband for the non-Doppler broadened spectra, Eq. (5) implies that the gain sideband will also be observed for the Doppler broadened co-propagating case. The same cannot be said for the counter-propagating case as Eq. (6) indicates a convolution of the spectral line-shape with the Gaussian velocity distribution that implies an averaging over the line-shape itself. This would still lead to a washing out of the gain sideband. To understand this discrepancy, we must understand the role of the relative Doppler shift in the velocity averaging.

#### IV. PERSISTENT STEADY STATE GAIN WITH DOPPLER BROADENING

From Eqs. (3) and (4), we note that the lab frame frequency  $\omega$  maps to a rest frame detuning  $\delta(\omega, v)$ . In the co-propagating case, for  $\Delta_P \gg \Delta_{\text{Dop}}$ , the relative Doppler shift



is zero and each  $\omega$  maps to a fixed detuning  $\delta(\omega) = \omega - \omega_P$  for every velocity. However, in the counterpropagating case, we instead have  $\delta(\omega, v) = \omega - \omega_P + 2\vec{k}_P \cdot \vec{v}$ . This implies, that provided a large enough spread of velocities, we can find an atom traveling with a velocity  $v$  such that  $\omega$  maps to a detuning  $\delta(v)$  that is within a peak in the spectral line-shapes. This suggests a broadening of the spectral line-shapes as well the possibility of inhomogeneous broadening that can overlap different peak features from different velocity groups. This also implies that we cannot remove the velocity group interference effect as we did for the co-propagating case. However, if we choose large enough  $\Omega_P$ , we can ensure that the gain sideband is far away from absorptive features such that we still observe a broadened gain feature for the counter-propagating case. We then refine our parameter conditions to  $\Omega_P > \Delta_P \gg \Delta_{\text{Dop}}$ . The presence of gain sidebands in  $g_A(\omega)$  for parameters that satisfy the aforementioned condition is shown in Fig. 6. We observe the expected gain sideband in the co-propagating case, which largely preserves the qualitative features of the sideband for the non-Doppler broadened case. The crucial result is the broadened gain sideband for the counter-propagating case, which confirms the predicted broadening due to convolution of the spectral response with the velocity distribution. The presence of peaks in the emission spectrum, corresponding to the gain sideband, demonstrates that the seeding radiation for the  $x$ -polarized light will be generated by spontaneous emission. For sufficiently large optical densities, optical gain in the vapor will lead to ASE and degenerate mirrorless lasing.

We remark that the degenerate mirrorless lasing we have discussed here occurs without the presence of a phase-stabilization feedback loop (such as those generated by mirrors in a cavity or strong scattering in random media). Even though a threshold behaviour has been observed with ASE for sufficiently large optical densities, it is still not settled whether the statistical properties of ASE, determined by the quantum statistics of spontaneous emission, would eventually change to the Poissonian statistics of coherent light while significantly above threshold. Theoretical simulations of the second-order coherence function,  $g^{(2)}(0)$  of ASE in a gain medium without feedback, utilizing stochastic equations for the atom and field operations with classical Langevin noise terms, show that  $g^{(2)}(0) \approx 2$  (super-Poissonian) for above-threshold conditions [11]. It was shown that inclusion of a feedback loop, through reflecting boundary conditions in the simulation, result in the expected coherent lasing behaviour  $g^{(2)}(0) \approx 1$  (Poissonian). Further study of the statistics of ASE in atomic vapor, both theoretically and experimentally, is needed to arrive at a more conclusive answer.

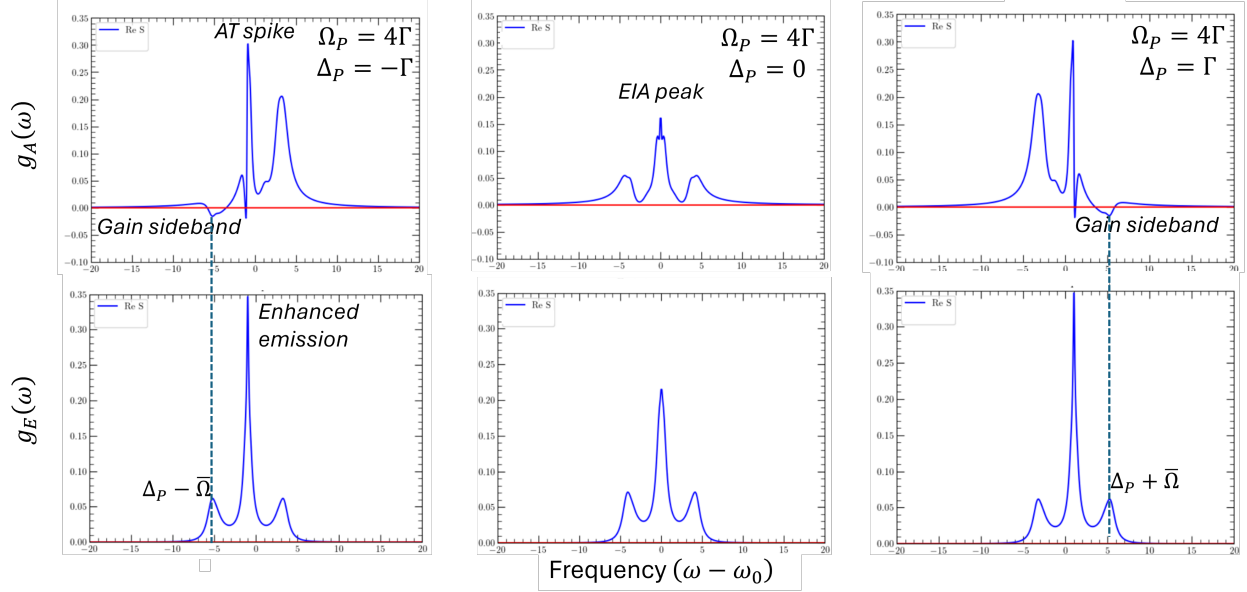


FIG. 4. Non Doppler-broadened spectral lineshapes for absorption (top) and emission (bottom) for strong driving ( $\Omega = 4\Gamma$ ) for different values of the pump detuning  $\Delta_P$ . The EIA peak feature is observed at resonant driving and gain sidebands and the AT spikes are observed for  $\Delta_P = \pm\Gamma$ .

## V. CONCLUSION

We considered the problem of degenerate mirrorless lasing in alkali atom vapors driven by continuous-wave linearly polarized light propagating along a single direction. We theoretically analyzed the steady-state dynamics, including the emission and absorption spectral lineshapes for orthogonally polarized light, under both ideal conditions and in the presence of Doppler broadening. We have demonstrated that the suppression of the gain sideband by Doppler broadening can be compensated by choosing detunings larger than the Doppler width and large Rabi frequencies, resulting in the generation of orthogonally polarized light in the backward and forward directions. Our results indicate that we can reproduce the observed optical gain in ultra-cold vapors and collimated atomic beams in the cold and warm vapor regimes. This will be of significant utility to experimentalists investigating remote sensing protocols, as the generation of backward-directed lasing in optically pumped remote samples can be used to simplify the experimental setup and provide an improvement to the signal-to-noise ratio and sensitivity.

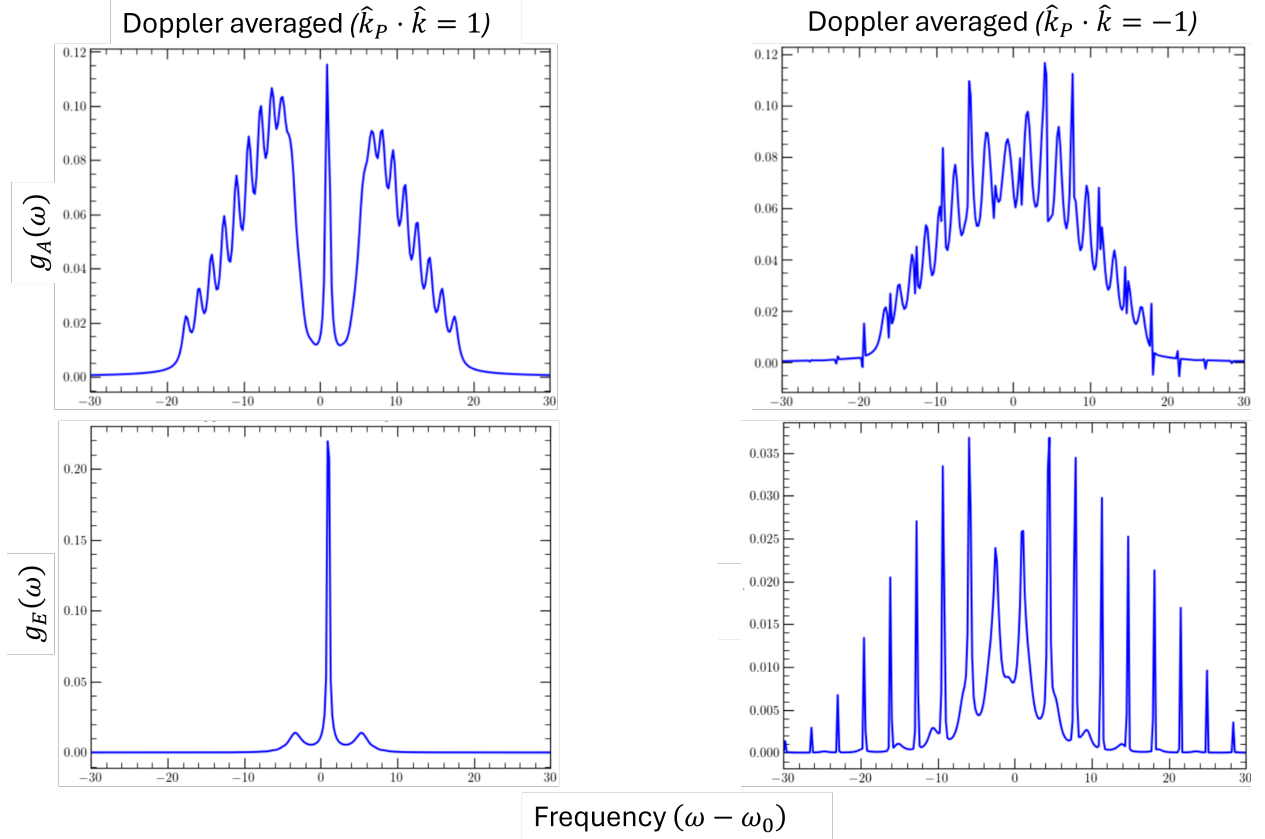


FIG. 5. Doppler broadened spectral lineshapes for absorption (top) and emission (bottom) for the co-propagating (left) and counter-propagating (right) cases. The parameters are  $\Omega_P = 4\Gamma$ ,  $\Delta_P = \Gamma$  and  $\Delta_{Dop} = 8.5\Gamma$ . For the calculation, 21 velocity classes were used for the Doppler averaging to demonstrate the effect of the relative Doppler shift in displacing the peaks from different velocity groups for the counter-propagating case.

### Appendix A: Dressed state analysis

We use the semiclassical dressed state formalism [12] to determine the eigenstates of  $H(\vec{v}) = \sum_m (\Delta_P(\vec{v})\sigma_m^z(\vec{v}) + \Omega_{P,m}\sigma_m^x(\vec{v}))$ . Since the pump only couples states with the same  $m$ -number, the eigenstates are the same as that for a system of uncoupled TLSs,

$$\begin{aligned}
 |+(v), m\rangle &= \cos(\theta_m(v)) |F = 2, m\rangle - \sin(\theta_m(v)) |F' = 3, m\rangle \\
 |-(v), m\rangle &= \sin(\theta_m(v)) |F = 2, m\rangle + \cos(\theta_m(v)) |F' = 3, m\rangle
 \end{aligned}
 \tag{A1}$$

Where  $\tan(2\theta_m(v)) = \Omega_{P,m}/\Delta_P(v)$  and the eigenenergy is given by the generalized Rabi frequency  $\bar{\Omega}_m = \sqrt{\Omega_{P,m}^2 + \Delta_P(v)^2}/2$ . The Hamiltonian is diagonal in this basis,  $H_D(v) =$

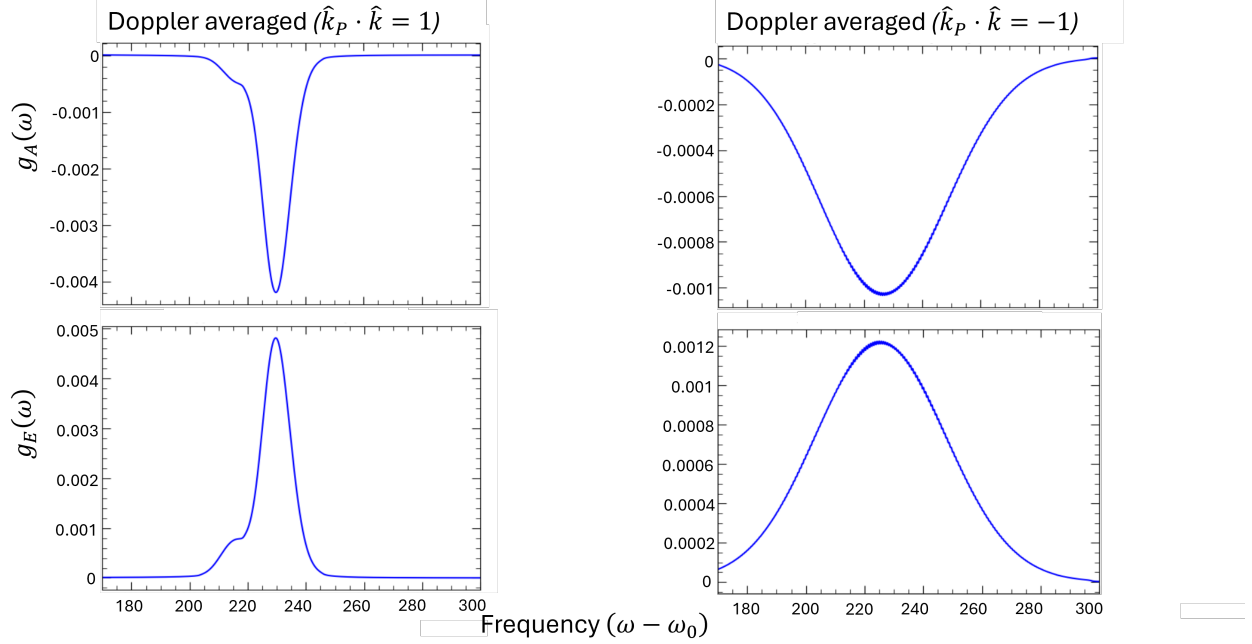


FIG. 6. Spectral lineshapes in the Doppler broadened spectra about the gain sideband region for the  $\Omega_P > \Delta_P \gg \Delta_{Dop}$  scheme. The absorption (top) and emission (bottom) lineshapes are given for the co-propagating (left) and counterpropagating (right) cases. Persistent steady state gain is achieved for both cases although there is still inhomogeneity with respect to the relative propagation  $\hat{k}_P \cdot \hat{k}$ . The parameters are  $\Omega_P = 120\Gamma$ ,  $\Delta_P = 80\Gamma$  and  $\Delta_{Dop} = 8.5\Gamma$ . For the velocity averaging procedure, 181 velocity classes were used.

$\sum_m \pm \bar{\Omega}_m |\pm(v), m\rangle \langle \pm(v), m|$  and we can expand the dipole lowering operators in the dressed state basis,

$$d^{z,-}(\vec{v}) = \sum_m \left( \frac{\sin(2\theta_m(v))}{2} (\mp |\pm, m\rangle \langle \pm, m|) \right. \\ \left. \cos^2(\theta_m(v)) |+, m\rangle \langle -, m| - \sin^2(\theta_m(v)) |-, m\rangle \langle +, m| \right) \quad (\text{A2})$$

$$d^{x,-}(\vec{v}) = \sum_m \left( -\cos(\theta_m(v)) \sin(\theta_{m\pm 1}(v)) |+, m\rangle \langle +, m \pm 1| \right. \\ \left. + \sin(\theta_m(v)) \cos(\theta_{m\pm 1}(v)) |-, m\rangle \langle -, m \pm 1| \right. \\ \left. + \cos(\theta_m(v)) \cos(\theta_{m\pm 1}(v)) |+, m\rangle \langle -, m \pm 1| \right. \\ \left. - \sin(\theta_m(v)) \sin(\theta_{m\pm 1}(v)) |-, m\rangle \langle +, m \pm 1| \right) \quad (\text{A3})$$

Introducing the dressed state expansion into Eq. (1), we see that the dissipators  $\mathcal{D}[d^{(\mu)-}(\vec{v})]$  couple many of the dressed states through incoherent processes. In this sense, the true dressed states for the open system are the eigenstates of the Lindbladian satisfying  $\mathcal{L}(v)\rho_{d,n}(v) = -(\gamma_{d,n} + i\nu_{d,n})\rho_{d,n}(v)$ . We now expand the dipole correlation functions (3) and (4) in the open system eigenbasis. We expand the dipole operators in this basis and define factors  $C_n[d^{(\mu),-}(\vec{v})] = \text{Tr}[d^{(\mu),+}(\vec{v})\rho_{d,n}(v)]$ . This converts the matrix superoperator exponential  $e^{(\mathcal{L}(v))^{\dagger}\tau}$  to a c-number. We then obtain,

$$g_E(\omega, v) = \sum_{n,n'} \frac{C_n[\rho_{ss}(\vec{v})d^{x,+}(\vec{v})]C_{n'}[d^{x,-}(\vec{v})]}{\gamma_{d,n} + i(\nu_{d,n} + \delta(\omega, v))} \text{Tr}[\rho_{d,n}(v)\rho_{d,n'}(\vec{v})] \quad (\text{A4})$$

$$g_A(\omega, v) = \sum_{n,n'} \frac{(C_n[d^{x,+}(\vec{v})\rho_{ss}(\vec{v})] - C_n[\rho_{ss}(\vec{v})d^{x,+}(\vec{v})])C_{n'}[d^{x,-}(\vec{v})]}{\gamma_{d,n} + i(\nu_{d,n} + \delta(\omega, v))} \text{Tr}[\rho_{d,n}(v)\rho_{d,n'}(\vec{v})] \quad (\text{A5})$$

These terms show that the spectral lineshapes are a sum of Lorentzians with central frequency  $\nu_{d,n} - \omega_P + (\vec{k}_P - \vec{k}) \cdot \vec{v}$  and full-width-at-half-maximum  $\gamma_{d,n}$ . If we want to determine the correspondence between each Lorentzian and the dressed states of  $H(\vec{v})$ , we can introduce the factor  $w_{\pm_1\pm_2}^{mm'}[d^{x,-}(\vec{v})] = \langle \pm_2(\vec{v}), m' | d^{x,+}(\vec{v}) | \pm_1(\vec{v}), m \rangle$  and obtain,

$$g_E(\omega, v) = \sum_{m,m'} w_{\pm_1\pm_2}^{mm'}[d^{x,-}(\vec{v})] \sum_n \frac{C_n[\rho_{ss}(\vec{v})d^{x,+}(\vec{v})] \langle \pm_2(\vec{v}), m' | \rho_{d,n}(\vec{v}) | \pm_1(\vec{v}), m \rangle}{\gamma_{d,n} + i(\nu_{d,n} + \delta(\omega, v))} \quad (\text{A6})$$

$$g_A(\omega, v) = \sum_{m,m'} w_{\pm_1\pm_2}^{mm'}[d^{x,-}(\vec{v})] \sum_n \frac{C_n[d^{x,+}(\vec{v})\rho_{ss}(\vec{v})] - C_n[\rho_{ss}(\vec{v})d^{x,+}(\vec{v})]}{\gamma_{d,n} + i(\nu_{d,n} + \delta(\omega, v))} \times \langle \pm_2(\vec{v}), m' | \rho_{d,n}(\vec{v}) | \pm_1(\vec{v}), m \rangle \quad (\text{A7})$$

In the limit of  $\Omega_P, |\Delta_P| \gg \Gamma$ , where the coherent dynamics dominate over the incoherent dynamics, the correspondence between the dressed states of the field interaction Hamiltonian and the Lindbladian is sufficient that we can assign each Lorentzian peak and  $\rho_{d,n}$  to a specific dressed state population or coherence.

---

[1] A. Ramaswamy, J. Chathanathil, D. Kanta, E. Klinger, A. Papoyan, S. Shmavonyan, A. Khanbekyan, A. Wickenbrock, D. Budker, and S. A. Malinovskaya, Mirrorless lasing: a theoretical perspective, *Optical Memory and Neural Networks* **32**, S443 (2023).

- [2] J. Mompert and R. Corbalán, Lasing without inversion, *Journal of Optics B: Quantum and Semiclassical Optics* **2**, R7 (2000).
- [3] N. Lu and P. R. Berman, Lasing without inversion in dressed-state lasers, *Phys. Rev. A* **44**, 5965 (1991).
- [4] Z. Ficek, W. Smyth, and S. Swain, Gain without population inversion in a two-level atom damped by a broadband squeezed vacuum, *Optics Communications* **110**, 555 (1994).
- [5] F. Y. Wu, S. Ezekiel, M. Ducloy, and B. R. Mollow, Observation of amplification in a strongly driven two-level atomic system at optical frequencies, *Phys. Rev. Lett.* **38**, 1077 (1977).
- [6] G. Khitrova, J. F. Valley, and H. M. Gibbs, Gain-feedback approach to optical instabilities in sodium vapor, *Phys. Rev. Lett.* **60**, 1126 (1988).
- [7] A. Lipsich, S. Barreiro, A. M. Akulshin, and A. Lezama, Absorption spectra of driven degenerate two-level atomic systems, *Phys. Rev. A* **61**, 053803 (2000).
- [8] A. M. Akulshin, D. Budker, F. Pedreros Bustos, T. Dang, E. Klinger, S. M. Rochester, A. Wickenbrock, and R. Zhang, Remote detection optical magnetometry, *Physics Reports* **1106**, 1 (2025), remote Detection Optical Magnetometry.
- [9] B. Mollow, Absorption and emission line-shape functions for driven atoms, *Physical Review A* **5**, 1522 (1972).
- [10] A. Lezama, S. Barreiro, A. Lipsich, and A. M. Akulshin, Coherent two-field spectroscopy of degenerate two-level systems, *Phys. Rev. A* **61**, 013801 (1999).
- [11] I. V. Doronin, E. S. Andrianov, A. A. Zyablovsky, A. A. Pukhov, Y. E. Lozovik, A. P. Vinogradov, and A. A. Lisiansky, Second-order coherence properties of amplified spontaneous emission, *Optics Express* **27**, 10991 (2019).
- [12] P. R. Berman and R. Salomaa, Comparison between dressed-atom and bare-atom pictures in laser spectroscopy, *Phys. Rev. A* **25**, 2667 (1982).